J. Fluid Mech. (1988), *vol.* 197, *pp.* 171–199
Printed in Great Britain

On direct methods in water-wave theory

By JONATHAN J. SHIELDS AND WILLIAM C. WEBSTER
Department of Naval Architecture and Offshore Engineering, University of California at Berkeley, CA 94720, USA

(Received 29 July 1986 and in revised form 10 May 1988)

Model equations for three-dimensional, inviscid flow between two arbitrary, time-varying material surfaces are derived using a 'direct' or variational approach due to Kantorovich. This approach results in a hierarchy of approximate theories, each of a higher level of spatial approximation and complexity. It can be shown that the equations are equivalent in substance to 'the theory of directed fluid sheets' of Green & Naghdi (1974, 1976).

The theory can be used to study the propagation of long waves in water of finite depth and, as such, competes with theories derived using the classical Rayleigh–Boussinesq perturbation methods. In order to demonstrate that there is an advantage to the present approach, we compare predictions for steady, two-dimensional waves over a horizontal bottom. Numerical solutions indicate that the direct theory converges more rapidly than the perturbation theories. Also, the equations of the higher-order direct theories contain singularities related to waves of limiting height, and indeed such waves can be predicted with relative accuracy. Finally, the range of applicability of the direct theory is far greater: waves as short as three times the water depth can be modelled. This is essentially a deep-water condition, well beyond the range of convergence of the Rayleigh–Boussinesq approach.

1. Introduction

Flows which may be characterized as thin or 'sheet-like' occur throughout nature and include, for example, lubrication and coating flows, jet and free-sheet flows (such as the flow over a waterfall), and the propagation of fairly long waves in a fluid of finite depth. In this paper we discuss an approximate nonlinear theory for treating such phenomena, focusing on wave propagation in an incompressible, inviscid medium as the primary application. We shall be concerned with problems of considerable generality: model equations appropriate for unsteady, three-dimensional flow with variable bathymetry will be derived. Our approach is very different from classical approaches to this problem, and results in equations that differ as well. Thus our primary objective has been to determine if the present theory has any advantage over these other more well-known methods.

Before describing the contribution of this paper, it seems appropriate to review briefly the classical approaches. There are two main approximation schemes commonly used, both based on expansions in a small parameter. The best known is that of Stokes (1847) where this parameter is the leading coefficient in a Fourier expansion of the wave profile, appearing in dimensionless form as $a_1 k$, where k is the wavenumber. Stokes carried out this procedure to the third order for the problem of two-dimensional waves propagating steadily over a horizontal bed. He noted that the approximation is most accurate when the wave height is not too large compared

with the length (i.e. $a_1 k \ll 1$) and that the convergence is slowed as the ratio of wavelength to depth increases. Fifth-order Stokes-type expansions have been given by De (1955), Skjelbreia & Hendrickson (1961) and Fenton (1985). Using numerical techniques, Schwartz (1974) and Cokelet (1977) carried out similar approximations to very high order, obtaining highly accurate solutions for all but the longest waves. Low-order Stokes' theory is most appropriate in deep-water wave problems. For the complementary case of long waves (or shallow water) a different procedure, usually associated with the works of Rayleigh (1876) and Boussinesq (1871, 1877), offers a better simple approximation. This procedure is a perturbation method based on two non-dimensional parameters: ϵ, the ratio of wave height to water depth, and σ, the ratio of depth to wavelength. Both parameters are assumed small and, as was clarified by Ursell (1953), relate to one another in such a way that $\epsilon/\sigma^2 = O(1)$. The theory differs from that of Stokes in that the lowest-order approximation results in a nonlinear differential equation for the wave profile. This equation possesses analytic solutions in terms of the Jacobian elliptic function cn, hence the approximation has become known as 'cnoidal wave theory'. Higher-order cnoidal approximations have been obtained, most notably the second-order theory of Laitone (1960), the third-order theory of Grimshaw (1971) and the computer-extended, high-order theories of Fenton (1972, 1979).

The general procedure of these shallow-water approximations is not limited to the case of steady waves, but can be extended to time-dependent problems as well. The simplest such 'evolution equation' is the Korteweg–de Vries (KdV) equation, which has been studied extensively. More complicated, higher-order models are also possible, such as a pair of equations attributed to Boussinesq. More recently, Su & Mirie (1980) have shown that it is possible to derive similar equations at any order of approximation. Within the framework of the theory one may also include the effects of variable bathymetry. Different approaches to this problem are represented by the works of Peregrine (1967), Madsen & Mei (1969), Miles (1979) and many others, including Wu (1981) who presents a complete unsteady, three-dimensional theory.

Perturbation methods are not, however, the only approach available for these problems. Using fundamental principles of continuum mechanics and making use of a special continuum model called a Cosserat or 'directed' surface. Green, Laws & Naghdi (1974) and Green & Naghdi (1976) developed a 'theory of directed fluid sheets'. This nonlinear theory models inviscid flow between two smooth, non-intersecting, time-varying material surfaces. Specializing the theory for the case of a fixed lower surface and a free upper surface, one obtains equations for surface-wave propagation over fixed bathymetry. The theory is most appropriate in the shallow-water or long-wave regime and, as such, competes most directly with the Rayleigh–Boussinesq-type approximations.

Yet another approach for sheet-like flows has been introduced by Russian workers. Levich & Krylov (1969, pp. 313–314) describe a variational or 'direct' method of approximation which they compare to the well-known moment method in the theory of laminar boundary layers. Although the ensuing applications appear to have been primarily for viscous and surface-tension-driven flows, the resulting equations are equivalent to an Eulerian version of the directed-fluid-sheet theory for a Newtonian fluid, presented by Green & Naghdi (1984). We note, however, that although one obtains the same equations for this special fluid, there is no guarantee that this will always be the case. In particular, the approach of Green & Naghdi forms a framework for treating fluids with complex rheology. This feature and other

differences between these two similar, yet distinct approaches are discussed by Antman (1972) in the context of the theory of rods.

Like the perturbation methods, the Cosserat surface approach (or, equivalently for Newtonian fluids, the variational approach) also yields a hierarchy of approximate theories, each of increasing complexity. Convergence of this hierarchy has not been established, nor even demonstrated numerically. Previous applications in inviscid-flow problems have thus far used only the lowest level of approximation in this hierarchy, the so-called 'restricted theory of a directed fluid sheet' (Green & Naghdi 1976). These applications include the transition to planning of a boat (Naghdi & Rubin 1981*a*), the flow over a waterfall (Naghdi & Rubin 1981*b*), soliton generation by a moving pressure disturbance (Ertekin 1984; Ertekin, Webster & Wehausen 1984, 1986), and the downstream flow past an obstacle, (Naghdi & Vongsarnpigoon 1986).

Miles & Salmon (1985) have provided an alternative means of obtaining the 'restricted-theory', basing their derivation on Hamilton's principle. They also explore the relationship between the restricted theory and earlier theories and show that, for the case of uniform depth, the equations are equivalent to a generalization of Boussinesq's equations (due to Whitham 1967) in which dispersion, but not nonlinearity, is assumed to be weak. The Boussinesq equations themselves may be obtained after a formal expansion (this has also been shown previously by Ertekin 1984). While the relationship between the Green–Naghdi and Boussinesq theories is certainly of interest, such results do not provide compelling reasons to prefer the former theory, especially since convergence of the Green–Naghdi approach remains an unanswered question.

This paper begins with a new derivation of the 'direct theory' (as we shall call it) for unsteady, inviscid flow. Our derivation, presented in §3, follows the approach of Levich & Krylov, but we find it possible to describe this more formally within the framework of a variational method due to Kantorovich (given in Kantorovich & Krylov 1958). We also introduce a special mapping that results in simplification of the fluid equations. It has been shown by Shields (1986) that these may be algebraically transformed to the Green–Naghdi (1984) equations, and are therefore equivalent in substance.

Premising that the worth of an approximate theory should be measured by its ability to describe the physical system it attempts to model, it is our intent to show that the direct theory does have a definite advantage over the theories of the Rayleigh–Boussinesq class. Thus, the remainder of the paper is devoted to a comparison of the predictive capability of the direct theory with the classical theories. In order to make this assessment, we note that the overall accuracy of a set of model equations can be no better than their accuracy for relatively simple, steady-state problems. With this in mind, we restrict attention to two-dimensional waves of permanent form in §§4–7, and use this problem as a benchmark for evaluating the two different types of approximation. We consider the first three hierarchical levels of the direct theory, specializing the equations for steady two-dimensional flow over a horizontal bottom. Solitary and periodic wave solutions for each level are obtained and are compared with a similar hierarchy of steady-state solutions from the competing Rayleigh–Boussinesq approximation. These include the results of Boussinesq (1871), Laitone (1960), Grimshaw (1971) and Fenton (1972, 1979). Exact and high-order numerical results of Stokes, Longuet-Higgins & Fenton (1974), Byatt-Smith & Longuet-Higgins (1976) and Cokelet (1977) provide an appropriate standard for this comparison.

Our numerical solutions suggest that the direct theory converges much more rapidly than the Rayleigh–Boussinesq theory, and that the range of applicability is far greater as well. In particular, the third-level approximation compares well with high-order numerical results even for rather short waves ($\sigma \approx \frac{1}{3}$). This is well beyond the range of applicability of even high-order cnoidal theory ($\sigma \leqslant \frac{1}{8}$ according to Fenton 1979). Finally, it is found that the phenomenon of limiting waves is implicit in the second and higher-level approximations; a singularity associated with waves of limiting height can be identified in the governing equations. In numerical solutions the predicted wave profiles become increasingly sharp crested as this singularity is approached, but eventually the numerics break down and no solution can be obtained. For the third-level approximation the point at which this occurs is very near to high-order numerical results for limiting wave height and speed.

2. Problem statement

Let (x^1, x^2, x^3) be a system of fixed, rectangular Cartesian coordinates with base vectors $(\boldsymbol{e}_1, \boldsymbol{e}_2, \boldsymbol{e}_3)$, where $\boldsymbol{e}_3$ is oriented vertically upwards. With reference to figure 1, we consider the motion of a sheet-like body of incompressible, inviscid fluid in a gravitational field $-g\boldsymbol{e}_3$. The fluid is assumed to be bounded from above and below by two smooth, non-intersecting, time-varying material surfaces

$$x^3 = \alpha(x^1, x^2, t), \quad x^3 = \beta(x^1, x^2, t), \quad \beta > \alpha. \tag{2.1}$$

The local thickness η and mid-surface location ζ are defined by

$$\eta(x^1, x^2, t) = \beta - \alpha, \quad \zeta(x^1, x^2, t) = \tfrac{1}{2}(\beta + \alpha). \tag{2.2}$$

In the following we shall use standard Cartesian-tensor notation, with the summation convention implied for repeated indices. Latin indices are used for quantities having three spatial components and take the values 1, 2, 3; Greek indices take the values 1, 2 only.

The equations of motion for the fluid body are the continuity equation and Euler's equations

$$v^i_{,i} = 0, \tag{2.3}$$

and

$$\boldsymbol{v}_{,t} + v^i \boldsymbol{v}_{,i} = -\frac{1}{\rho} p_{,t} \boldsymbol{e}_i - g\boldsymbol{e}_3, \tag{2.4}$$

respectively, where $\boldsymbol{v} = v^i(x^1, x^2, x^3, t)\,\boldsymbol{e}_i$ is the fluid velocity and where $p(x^1, x^2, x^3, t)$ is the pressure.

The principal of equivalence of external and internal pressures at the surfaces α and β yields dynamic boundary conditions

$$p|_{x^3=\beta} = \hat{p}, \quad p|_{x^3=\alpha} = \bar{p}, \tag{2.5}$$

where $\hat{p}$ and $\bar{p}$ are the pressures acting on the upper and lower surfaces, respectively. Kinematic boundary conditions follow from the hypothesis that α and β are material surfaces, which imposes the constraint that the vertical velocity of surface particles is identical to that of the surfaces themselves. Thus,

$$[v^3 - \alpha_{,t} - v^\gamma \alpha_{,\gamma}]|_{x^3=\alpha} = 0, \tag{2.6a}$$

and

$$[v^3 - \beta_{,t} - v^\gamma \beta_{,\gamma}]|_{x^3=\beta} = 0. \tag{2.6b}$$

This problem statement is completed by additional boundary conditions on the (as yet unspecified) vertical control surfaces closing the domain.

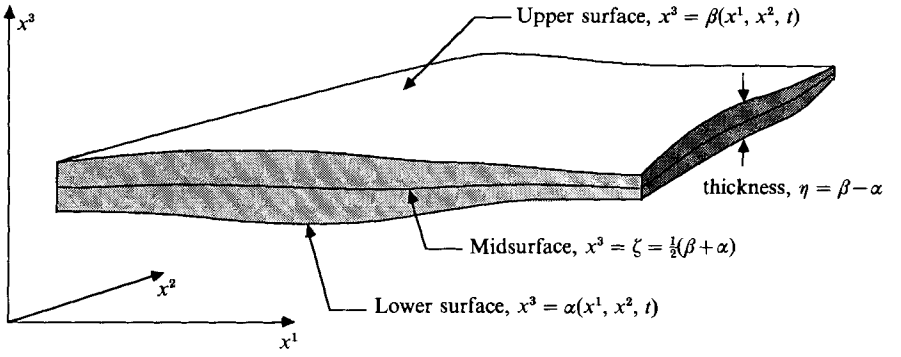

FIGURE 1. Definition sketch: a thin fluid body bounded by two material surfaces.

3. Derivation of approximate equations by the method of Kantorovich

We wish to take advantage of the sheet-like geometry of the fluid body in order to obtain model equations that depend on only two spatial coordinates, x^1 and x^2. Our approach follows the 'method for reduction to ordinary differential equations' of Kantorovich, given by Kantorovich & Krylov (1958). This approach is a variational method similar to that of Ritz and Galerkin, but seeks to reduce the dimensionality of a system of partial differential equations, rather than to replace the system with algebraic equations. The fundamental idea is to assume a form for the solution in the spatial direction to be eliminated (in the present case, $\boldsymbol{e}_3$). This form must be chosen such that the boundary conditions can be satisfied, and must incorporate coefficients that are undetermined functions of the remaining independent variables (i.e. the horizontal coordinates). A variational procedure is then used to minimize the error when this constrained solution is introduced into the original equations, yielding equations for the undetermined coefficients.

In the present application, we select a solution for the velocity field which assumes a finite power-series form for the variation in the vertical direction. Before writing this explicity, it is advantageous to first introduce the following transformation:

$$s(x^1, x^2, x^3, t) = (2/\eta)\,(x^3 - \zeta). \tag{3.1}$$

As defined, the function s maps the physical fluid body to a region between two parallel planes in the coordinate system (x^1, x^2, s), given by $|s| \leqslant 1$. In particular, the upper surface of the fluid ($x^3 = \beta$) is mapped to $s = +1$, the lower surface is mapped to $s = -1$, and the midsurface is mapped to $s = 0$.

Let us now assume a solution for the velocity field of the form

$$\boldsymbol{v}(x^1, x^2, x^3, t) = \sum_{n=0}^{K} \boldsymbol{W}_n(x^1, x^2, t)\, s^n, \tag{3.2}$$

where the coefficients $\boldsymbol{W}_n\,(= W_n^i(x^1, x^2, t)\,\boldsymbol{e}_i)$ are unknown time-dependent vector fields defined over the (x^1, x^2)-plane. The number of terms in the series, and hence the complexity of the spatial representation, is determined by the positive integer K, which we leave unspecified. Each choice $K \geqslant 1$ will yield a complete set of equations forming one member of a hierarchy of approximate theories. In this paper we shall refer to a particular member of this hierarchy as the 'ith level approximation' or simply 'Theory i' for $K = i$ in (3.2).

We now must find equations to determine the $\boldsymbol{W}_n$. To begin, we require that the kinematic boundary conditions be satisfied. Introducing the approximation (3.2) into (2.6), we obtain the following two equations:

$$2\sum_{n=1,3}^{K} W_n^3 = \eta_{,t} + \eta_{,\gamma}\sum_{n=0,2}^{K} W_n^\gamma + 2\zeta_{,\gamma}\sum_{n=1,3}^{K} W_n^\gamma, \tag{3.3a}$$

$$2\sum_{n=0,2}^{K} W_n^3 = 2\zeta_{,t} + \eta_{,\gamma}\sum_{n=1,3}^{K} W_n^\gamma + 2\zeta_{,\gamma}\sum_{n=0,2}^{K} W_n^\gamma. \tag{3.3b}$$

We also shall require that mass be conserved at each point in the domain. Thus we substitute (3.2) into the continuity equation (2.3), and equate coefficients of powers of s to zero, obtaining

$$\dot{\zeta}_{,\gamma} W_n^\gamma + \tfrac{1}{2}\eta_{,\gamma} W_{n-1}^\gamma - W_n^3 = \frac{1}{2n}(\eta W_{n-1}^\gamma)_{,\gamma} \quad \text{for} \quad n = 1, 2, \ldots, K, \tag{3.4a}$$

and

$$W_K^\gamma = 0 \tag{3.4b}$$

(Equation (3.4b) states that the Kth term in the expansion has components in the $\boldsymbol{e}_3$ direction only. Green & Naghdi refer to such a component as a 'restricted director'.)

From the foregoing we see that the prescribed form for the velocity field (3.2) is capable of satisfying the kinematic requirements of an inviscid flow. However, when we substitute (3.2) for $\boldsymbol{v}$ in the Euler equations a difficulty arises. Taking (3.4b) into consideration, the left-hand sides of the $\boldsymbol{e}_1$ and $\boldsymbol{e}_2$ components of (2.4) will be polynomials in s of degree $2K-2$. If the equations are to hold everywhere within the fluid, the right-hand sides imply that the pressure p must also be a polynomial in s of degree $2K-2$.

Now consider the $\boldsymbol{e}_3$ component of (2.4). After using (3.2) for v^3 the left-hand side will be a polynomial in s of degree $2K-1$. The right-hand side of this equation, in turn, implies that p must be a polynomial of degree $2K$. Thus, a contradiction is encountered as to the dependence of p on s. This demonstrates that the kinematic assumption (3.2) is generally incapable of satisfying both the kinematic and dynamic requirements.

At this point we make the approximation. We shall seek equations such that momentum will be conserved in an approximate sense, using the 'weak' variational formulation of Kantorovich. In particular, we construct depth-averaged moments of the Euler equations, using the basis functions of the series (3.2) as weighting functions. These equations may be written as

$$\int_\alpha^\beta [\boldsymbol{v}_{,t} + v^i \boldsymbol{v}_{,i}]\, s^n \,\mathrm{d}x^3 = -\frac{1}{\rho}\int_\alpha^\beta [p_{,i}\boldsymbol{e}_i + \rho g \boldsymbol{e}_3]\, s^n \,\mathrm{d}x^3, \tag{3.5}$$

$$\text{for} \quad n = 0, 1, \ldots, K.$$

The above $K+1$ vector-valued relationships are sufficient to close the system of equations, and to determine all of the unknown $\boldsymbol{W}_n$. We now transform these equations into a more convenient form.

First using (3.2) in the left-hand sides of (3.5), and rearranging the right-hand sides, we have

$$\int_\alpha^\beta \sum_{m=0}^{K} [(\boldsymbol{W}_m s^m)_{,t} + v^i(\boldsymbol{W}_m s^m)_{,i}] s^n \, dx^3$$
$$= -\frac{1}{\rho}\left[\int_\alpha^\beta (ps^n)_{,i}\, dx^3 - \int_\alpha^\beta nps^{n-1}s_{,i}\, dx^3\right]\boldsymbol{e}_i - \left[\int_\alpha^\beta gs^n\, dx^3\right]\boldsymbol{e}_3,$$
$$\text{for} \quad n = 0, 1, \ldots, K.$$

Leibnitz's rule is applied to the $\boldsymbol{e}_\gamma$ components of the first integral in the right-hand side of the above, and the $\boldsymbol{e}_3$ component can be integrated directly. After carrying out these operations and rearranging both sides, we obtain

$$\int_\alpha^\beta \sum_{m=0}^{K} [\boldsymbol{W}_{m,t} + v^\gamma \boldsymbol{W}_{m,\gamma}] s^{m+n}\, dx^3 + \int_\alpha^\beta \sum_{m=0}^{K} m\boldsymbol{W}_m [s_{,t} + v^i s_{,i}] s^{m+n-1}\, dx^3$$
$$= \left[\left[\int_\alpha^\beta ps^n\, dx^3\right]_{,\gamma} - \hat{p}\beta_{,\gamma} + (-)^n \bar{p}\alpha,\gamma - n\int_\alpha^\beta ps^{n-1}s_{,\gamma}\, dx^3\right]\boldsymbol{e}_\gamma$$
$$-\left[n\int_\alpha^\beta ps^{n-1}s_{,3}\, dx^3 + [\hat{p} - (-)^n\bar{p}] - \int_\alpha^\beta gs^n\, dx^3\right]\boldsymbol{e}_3, \quad (3.6)$$
$$\text{for} \quad n = 0, 1, \ldots, K.$$

From the definition (3.1) we note that

$$s_{,3} = \frac{2}{\eta}, \quad s_{,\gamma} = \frac{-1}{\eta}[\eta_{,\gamma}s + 2\zeta_{,\gamma}], \quad (3.7)$$
$$s_{,t} = \frac{-1}{\eta}[\eta_{,t}s + 2\zeta_{,t}],$$

and the material time derivative of the mapping s may be written

$$s_{,t} + v^i s_{,i} = (2/\eta)[v^3 - \zeta_{,t} - v^\gamma\zeta_{,\gamma} - (s/2)\eta_{,t} - (s/2)v^\gamma\eta_{,\gamma}].$$

We introduce the expansion for the velocity (3.2) into the above and also make use of the kinematic boundary conditions (3.3). After algebraic manipulation, the resulting expression may be further simplified with the use of (3.4). The final expression is

$$s_{,t} + v^i s_{,i} = \sum_{n=1}^{K} \frac{1}{n\eta}(\eta W^\gamma_{n-1})_{,\gamma}(s^{\pi(n)} - s^n), \quad (3.8)$$

where

$$\pi(n) = \begin{bmatrix} 0, & n \text{ even} \\ 1, & n \text{ odd} \end{bmatrix}. \quad (3.9)$$

(Note that (3.8) implies that a particle on the top or bottom surface ($s = \pm 1$) remains on the surface, ($s_{,t} + v^i s_{,i} = 0$), as required by the kinematic surface conditions.)

We can now eliminate all dependence on x^3 from the momentum conditions (3.6). We use (3.3) once again to eliminate v^γ from the left-hand sides, (3.7) and (3.8) to

eliminate all derivatives of s. After interchange of the orders of summation and integration, the resulting expressions may be written as

$$\sum_{m=0}^{K}\left[\eta\theta_{m+n}[\boldsymbol{W}_{m,t}+W_0^{\gamma}\boldsymbol{W}_{m,\gamma}]+\sum_{r=1}^{K-1}\theta_{m+n+r}[\eta W_r^{\gamma}\boldsymbol{W}_{m,\gamma}+m\mu_{m+n}^{r}(\eta W_r^{\gamma})_{,\gamma}\boldsymbol{W}_m]\right]$$

$$=-\frac{1}{\rho}\left[P_{n,\gamma}+\frac{nP_n\eta_{,\gamma}}{\eta}+\frac{2nP_{n-1}\zeta_{,\gamma}}{\eta}-\hat{p}\beta_{,\gamma}+(-)^n\bar{p}\alpha_{,\gamma}\right]\boldsymbol{e}_{\gamma}$$

$$-\frac{1}{\rho}\left[\hat{p}-(-)^n\bar{p}-\frac{2nP_{n-1}}{\eta}+\theta_n\rho g\eta\right]\boldsymbol{e}_3$$

$$\text{for}\quad n=0,1,\ldots,K, \tag{3.10}$$

where we have denoted the integrals in (3.6) involving pressure terms by

$$P_i\equiv\int_{\alpha}^{\beta}ps^i\,\mathrm{d}x^3=\tfrac{1}{2}\eta\int_{-1}^{+1}ps^i\,\mathrm{d}s, \tag{3.11}$$

and have defined two sets of constants:

$$\theta_i\equiv\eta^{-1}\int_{\alpha}^{\beta}s^i\,\mathrm{d}x^3=\frac{1}{2}\int_{-1}^{+1}s^i\,\mathrm{d}s=\begin{bmatrix}1/(i+1) & i\ \text{even}\\ 0 & i\ \text{odd}\end{bmatrix} \tag{3.12}$$

and

$$\mu_i^r\equiv\begin{bmatrix}1/i & r\ \text{odd}\\ r/[(r+1)(i+1)] & r\ \text{even}\end{bmatrix}. \tag{3.13}$$

Note that the 'integrated pressure' P_K only appears in the $\boldsymbol{e}_{\gamma}$ components of the Kth momentum condition ((3.10) with $n=K$). These two equations effectively define the gradients of P_K in the $\boldsymbol{e}_1$ and $\boldsymbol{e}_2$ directions. We shall not concern ourselves with P_K and will omit it along with these associated equations from further developments. Also eliminating W_K^{γ} by (3.4b), what remains is a system of $4K+3$ scalar equations in $4K+5$ variables for each choice of $K\geqslant 1$. The variables are the $3K+1$ velocity components ($\boldsymbol{W}_n$, for $n=0,1,\ldots,K-1$ and W_K^3), K integrated pressures ($P_i, i=0,1,\ldots,K-1$), pressures on the upper and lower surfaces $\hat{p}$ and $\bar{p}$, the fluid thickness η, and the midsurface location ζ (recall that η and ζ are related to α and β by the relations (2.2)). The equations are the two kinematic boundary conditions (3.3), K continuity conditions (3.4a), K vector momentum equations ((3.10), $n=0,1,\ldots,K-1$) and 1 scalar momentum equation ((3.10), $n=K,\boldsymbol{e}_3$ component). Different physical situations, including fixed, free or prescribed-motion boundaries, are specified by fixing any two values of surface pressure ($\hat{p},\bar{p}$) or surface location (α,β). This completes the system, which may then be reduced to a smaller, more convenient set of governing equations.

The foregoing derivation can be further generalized by delaying any constitutive assumption and using the general Eulerian equations for conservation of mass and momentum as a starting point, rather than (2.3) and (2.4). This derivation is given by Shields (1986) in which it is shown that the resulting equations may be transformed to those of Green & Naghdi (1984).

Before proceeding, it is worth mentioning some important features of these equations. In contrast to perturbation theories, we have made no *a priori* restrictions on the sizes of any parameters and all nonlinear terms arising in the derivation process have been retained. One result is that the equations, like the physical laws

from which they are derived, remain invariant with respect to coordinate frame. Destruction of invariance frequently occurs in perturbation schemes when one neglects 'small' parameters. Green & Naghdi (1977) discuss this in detail and cite the Boussinesq and KdV equations as examples.

On the other hand, since the approximation scheme is not based on a 'smallness' assumption, the parameter range where it might be appropriate (i.e. small wave height, weak dispersion, etc.) is not immediately apparent. However, since the solution is guaranteed to satisfy kinematic boundary conditions, conservation of mass and depth-averaged conservation of momentum (conservation of depth-averaged energy may also be demonstrated, but we shall not do this here), we might expect reasonable predictions in situations where the assumed form for the velocity field does not differ significantly from physical reality.

4. Equations for steady two-dimensional waves

In order to assess the accuracy of this approximation, it is desirable to compare its predictions with those from competing approximate schemes by using exact and/or high-order numerical solutions as a standard of comparison. This is the objective we shall now pursue, restricting attention to the problem of symmetric, progressive gravity waves in water of uniform depth as a 'test case'.

At this point it is convenient to drop the Cartesian-tensor notation. Let us denote

$$\left.\begin{aligned} x \equiv x^1, \quad z \equiv x^3, \\ u_n \equiv W_n^1, \quad w_n \equiv W_n^3, \end{aligned}\right\} \tag{4.1}$$

and also non-dimensionalize the variables by choosing units of length, mass and time such that

$$g = L = \rho = 1, \tag{4.2}$$

where L is some characteristic length, to remain unspecified for the time being.

We now specialize the general equations of §3 for steady two-dimensional flow over a horizontal bottom. We choose coordinate axes (x, z) to be translating in the x-direction at wave speed such that the flow is independent of time. The x-axis is taken to lie on a level bottom so that the location of the bottom surface of the fluid is simply

$$\alpha(x) = 0. \tag{4.3}$$

The upper surface $\beta(x)$ is the free surface. With our choice of reference frame its location is numerically equal to the fluid thickness, and the midsurface location is half of this value, i.e.

$$\beta(x) = \eta(x), \tag{4.4}$$

$$\zeta(x) = \tfrac{1}{2}\eta(x). \tag{4.5}$$

Like the exact formulation for an incompressible fluid, the equations are indeterminate to within a constant additive pressure. Thus the free-surface condition may be effected by setting

$$\hat{p}(x) = 0 \tag{4.6}$$

without loss of generality.

4.1. *Theory I equation for steady two-dimensional flow*

We first obtain explicit equations for the first level of approximation, corresponding to $K = 1$ in the general equations. The result will be equivalent to the steady-state form of the 'restricted theory of a directed fluid sheet' of Green & Naghdi (1976).

By (3.2) and (3.4b), this level of approximation corresponds to a depth-independent horizontal velocity and a linear profile for the vertical velocity, given by

$$v^1 = u_0, \tag{4.7a}$$

$$v^3 = w_0 + w_1 s. \tag{4.7b}$$

Making use of the two-dimensional steady-flow assumptions set forth above, and setting $K = 1$ in (3.3), (3.4) and (3.10), we obtain a system of seven coupled equations. First, from (3.3) and (3.4b) we may write the two kinematic boundary conditions as

$$2w_0 = \eta_x u_0, \quad 2w_1 = \eta_x u_0, \tag{4.8a, b}$$

and from (3.4a) we obtain a continuity condition

$$\eta u_{0x} + 2w_1 = 0. \tag{4.9}$$

Conditions for conservation of momentum are obtained from (3.10). We write these in component form as follows:

$n = 0, x$-component:

$$\eta[u_0 u_{0x}] = -P_{0x}, \tag{4.10a}$$

$n = 0, z$-component:

$$\eta[u_0 w_{0x}] = \bar{p} - \eta, \tag{4.10b}$$

$n = 1, z$-component:

$$\eta[\tfrac{1}{3}u_0 w_{1x}] = -\bar{p} + 2/\eta P_0. \tag{4.10c}$$

Let us now simplify the remaining system of equations. First, eliminating w_1 between (4.8b) and (4.9) and integrating the resulting expression, we obtain

$$u_0 = Q/\eta, \tag{4.11}$$

where Q is a constant of integration. From the form of the above, it is clear that this constant is the mass flux per unit span, consistent with the kinematic assumption of the theory. From (4.8a, b) and (4.11) it follows that

$$w_0 = w_1 = \tfrac{1}{2}Q\eta_x/\eta. \tag{4.12}$$

With the use of (4.11), the first momentum equation (4.10a) becomes

$$-Q^2\eta_x/\eta^2 = -P_{0x},$$

which may be integrated to obtain

$$Q^2\eta^{-1} = -P_0 + S, \tag{4.13}$$

where S is a constant of integration. This equation represents conservation of depth-integrated horizontal momentum and we may identify the constant S with the momentum flux per unit span (corrected for pressure force and divided by the density), as defined by Benjamin & Lighthill (1954). Eliminating $\bar{p}$ between (4.10b) and (4.10c) and using (4.11) and (4.12), we obtain

$$\tfrac{2}{3}Q^2(\eta_x/\eta)_x = -\eta + 2/\eta P_0. \tag{4.14}$$

Eliminating P between the above and (4.13) yields

$$Q^2\eta^{-2} + \tfrac{1}{3}Q^2(\eta_x/\eta)_x = \eta^{-1}S - \tfrac{1}{2}\eta. \tag{4.15}$$

Upon multiplying the above by η_x/η, each term may be integrated and, after rearranging, the resulting expression is

$$\tfrac{1}{3}Q^2\eta_x^2+\eta^3-2R\eta^2+2S\eta-Q^2=0, \tag{4.16}$$

where R is a third constant of integration. It is remarkable that this equation is identical to the governing equation of classical cnoidal-wave theory (see for example Benjamin & Lighthill 1954), especially when one considers the vast difference between the direct and the perturbation approaches. There are significant differences between the solution for the velocity field associated with (4.16) from the two different approaches, however. Examination of these differences lends insight into the differences between the two theories.

For the direct theory the form of the velocity field was specified *a priori*, the horizontal component being constant through the depth and the vertical component varying linearly. Equations relating these components were obtained by insisting that mass be conserved and kinematic boundary conditions (on both the bottom and free surface) be satisfied. It is interesting that the very simple form chosen for the velocity can satisfy the kinematics of the cnoidal wave, while at the same time conserving depth-averaged horizontal and vertical momentum. We note, however, that the flow is not necessarily irrotational. In particular, it follows from (3.7*b*), (4.11) and (4.12) that the vorticity $\Omega(=v_2^1-v_x^2)$ varies linearly through the depth, given by

$$\Omega = Q\frac{2\eta_x^2-\eta\eta_{xx}}{2\eta^2}(1+s). \tag{4.17}$$

Thus the maximum vorticity is at the surface ($s=1$) and it is always zero at the bottom ($s=-1$). The vorticity is zero everywhere when the upper surface is horizontal, i.e. uniform flow.

The fact that the solutions of this theory will generally be rotational highlights the unusual nature of the approximation. It is not surprising, since we made no formal requirement that the flow be irrotational in the derivation process. We recall that irrotationality is not an intrinsic property of an inviscid flow. It is conservation of circulation (the Hankel–Kelvin Theorem) which *results* from the Euler equations that is often used together with an additional assumption of an initially irrotational fluid field to postulate irrotational flow. This, in turn, allows one to take advantage of the mathematical simplifications afforded by potential theory.

Such an approach is taken by Benjamin & Lighthill (1954) in their derivation of classical cnoidal theory. Irrotationality is assumed in order to guarantee the existence of a harmonic stream function. This is expanded in an infinite series containing unknown functions of the horizontal coordinate, and is constructed in such a way that the bottom boundary condition is satisfied by each term. The series is substituted into the free-surface boundary condition and an equation defining the momentum-flux per unit span. In the process of solving these equations, the series is truncated after N terms. Computation of the vorticity reveals a non-zero contribution arising from the Nth term. Thus, strictly speaking, neither momentum, the free-surface boundary condition nor irrotationality is satisfied exactly unless an infinite number of terms is used. Rather, they are all approximated in a consistent sense. One result is that the solution for the wave profile is not guaranteed to be a streamline of the flow described by the solution for the velocity field. Since the stream function is expanded about a uniform flow, we expect this sort of error to increase with the wave height.

Unlike the perturbation theory, the direct theory gives certain physical requirements greater importance than others. In particular, the solution for the velocity field is guaranteed to satisfy both conservation of mass and the free-surface boundary conditions on the solution for the wave profile exactly for all wave heights. In this sense, one might say that the direct theory produces a 'self-consistent' solution. This is only possible by placing more importance on satisfaction of these specific kinematic requirements and allowing the Euler equations to be satisfied only in a depth-averaged sense (in a fashion which assures, however, that the model conserves total mechanical energy).

In summary, it might be said that the perturbation approach is motivated by the belief that it is of primary importance to satisfy all equations to the same order of approximation. In this sense it is a *mathematical* approximation to the 'exact' equations. In contrast, the direct approach concentrates on satisfaction of the fundamental kinematics and averaged momentum, in order to develop a model that is self-consistent and physically reasonable. Thus, the direct approach might be thought of as a *physical* approximation. Although it is interesting to debate the relative merits of the foundations of these two approaches, it is probable that a definitive answer can be obtained only by comparing predictions of the two theories, as we shall undertake in §§5 and 6.

4.2. *Theory II equations for steady two-dimensional flow*

The second level of approximation of the direct theory is obtained by setting $K = 2$ in the general equations of §3. By (3.2) and (3.4*b*), a linear profile for the horizontal velocity and a parabolic profile for the vertical velocity are assumed. These are

$$v^1 = u_0 + u_1 s, \tag{4.18a}$$

$$v^3 = w_0 + w_1 s + w_2 s^2. \tag{4.18b}$$

Again making use of steady two-dimensional flow assumptions, we obtain a system of ten coupled equations. First, from (3.3) and (3.4*b*) we may write the two kinematic boundary conditions as

$$2w_0 + 2w_2 = \eta_x(u_0 + u_1), \tag{4.19a}$$

$$2w_1 = \eta_x(u_0 + u_1), \tag{4.19b}$$

and from (3.4*a*) we obtain two continuity conditions:

$$\eta u_{0x} - \eta_x u_1 + 2w_1 = 0, \tag{4.20a}$$

$$\eta u_{1x} - \eta_x u_1 + 4w_2 = 0. \tag{4.20b}$$

From (3.10) we obtain five momentum equations as follows:

$n = 0, x$-component:

$$\eta[u_0 u_{0x} + \tfrac{1}{3}u_1 u_{1x} + \tfrac{1}{3}u_1 \eta^{-1}(\eta u_1)_x] = -P_{0x}, \tag{4.21a}$$

$n = 0, z$-component:

$$\eta[u_0 w_{0x} + \tfrac{1}{3}u_1 w_{1x} + \tfrac{1}{3}w_1 \eta^{-1}(\eta u_1)_x + \tfrac{1}{3}u_0 w_{2x}] = \bar{p} - \eta, \tag{4.21b}$$

$n = 1, x$-component:

$$\eta[\tfrac{1}{3}u_0 u_{1x} + \tfrac{1}{3}u_1 u_{0x}] = -P_{1x} - \eta_x/\eta(P_1 + P_0), \tag{4.21c}$$

$n = 1, z$-component:

$$\eta[\tfrac{1}{3}u_0 w_{1x} + \tfrac{1}{3}u_1 w_{0x} + \tfrac{1}{5}u_1 w_{2x} + \tfrac{2}{15}w_2 \eta^{-1}(\eta u_1)_x] = -\bar{p} + 2/\eta P_0, \tag{4.21d}$$

$n = 2$, z-component:

$$\eta[\tfrac{1}{3}u_0 w_{0x} + \tfrac{1}{5}u_1 w_{1x} + \tfrac{1}{15}w_1 \eta^{-1}(\eta u_1)_x + \tfrac{1}{5}u_0 w_{2x}] = \bar{p} + 4/\eta P_1 - \tfrac{1}{3}\eta. \tag{4.21e}$$

This rather cumbersome system is now reduced to a more convenient system of two equations. Using (4.19) and (4.20), the velocity components u_n, w_n are all expressible in terms of the free-surface height η, the linear component of the horizontal velocity u_1, and the mass flux Q, which again arises as a constant of integration. The relations are

$$u_0 = Q/\eta, \quad w_0 = \tfrac{1}{4}(\eta u_1)_x + \tfrac{1}{2}(Q\eta_x/\eta), \tag{4.22a, b}$$

$$w_1 = \tfrac{1}{2}\eta_x(u_1 + Q/\eta), \quad w_2 = \tfrac{1}{4}(\eta_x u_1 - \eta u_{1x}). \tag{4.22c, d}$$

With the use of (4.22a), the first momentum equation (4.21a) becomes

$$-Q^2\eta_x/\eta^2 + \tfrac{1}{3}(\eta u_1 u_{1x} + u_1(\eta u_1)_x) = -P_{0x},$$

which may be integrated to obtain

$$Q^2\eta^{-1} + \tfrac{1}{3}\eta u_1^2 = -P_0 + S, \tag{4.23}$$

where S arises as a constant of integration and has the same physical significance as before.

Taking suitable algebraic combinations of (4.23), (4.21b–e), and derivatives thereof, we can eliminate all of the unknown integrated pressures P_i and bottom pressure $\bar{p}$ from the system. After using the relations (4.22) in the resulting equations, we arrive at a pair of coupled, ordinary differential equations for the free-surface height η and the linear component of horizontal velocity, u_1. These are

$$[9u_1^2\eta^3 + 25Qu_1\eta^2 + 20Q^2\eta]\eta_{xx} + [u_1\eta^4 + 5Q\eta^3]u_{1xx} + (6u_1^2\eta^2 - 5Qu_1\eta - 20Q^2)(\eta_x)^2 + (15u_1\eta^3 + 25Q\eta^2)u_{1x}\eta_x - \eta^4(u_{1x})^2 + 30\eta^3 + 20u_1^2\eta^2 - 60S\eta + 60Q^2 = 0, \tag{4.24}$$

and

$$[-u_1^2\eta^4 - 4Qu_1\eta^3 - 5Q^2\eta^2]\eta_{xxx} - [2Q\eta^4]u_{1xxx} + ((2u_1^2\eta^3 + 15Qu_1\eta^2 + 25Q^2\eta)\eta_x + (-5u_1\eta^4 - 11Q\eta^3)u_{1x})\eta_{xx} + (-2u_1\eta^4 - 8Q\eta^3)\eta_x u_{1xx} + (2u_1^2\eta^2 - 6Qu_1\eta - 20Q^2)(\eta_x)^3 + (2u_1\eta^3 + 10Q\eta^2)u_{1x}(\eta_x)^2 + (-4\eta^4(u_{1x})^2 - 20Qu_1\eta)\eta_x + 20Q\eta^2 u_{1x} = 0. \tag{4.25}$$

Upon setting u_1 to zero in (4.24) one recovers the first-level equation (4.16). It may be shown that the second equation, (4.25), is an additional requirement which cannot be satisfied by the more restricted velocity field associated with the first-level approximation, excepting trivial cases.

The depth–vorticity distribution of Theory II is determined by taking the curl of the velocity field defined by (4.18) and (4.22). The result is parabolic in the coordinate s, given by

$$\begin{aligned}\Omega = &-[\{u_1\eta^2\eta_{xx} - 2u_1\eta(\eta_x)^2 + 2u_{1x}\eta^2\eta_x - u_{1xx}\eta^3\}s^2 \\ &+ \{(2\eta\eta_{xx} - 4(\eta_x)^2)Q + 2u_1\eta^2\eta_{xx} - 4u_1\eta(\eta_x)^2 + 4u_{1x}\eta^2\eta_x\}s \\ &+ (2\eta\eta_{xx} - 4(\eta_x)^2)Q + u_1\eta^2\eta_{xx} - 2u_1\eta(\eta_x)^2 + 2u_{1x}\eta^2\eta_x + u_{1xx}\eta^3 - 8u_1\eta]/(4\eta^2).\end{aligned} \tag{4.26}$$

4.3. *Theory III equations for steady two-dimensional flow*

The equations for the third-level approximations are obtained by direct extension. We shall not dwell on this process, but record here only the results; a system of three coupled equations:

$$
\begin{aligned}
&[(567u_1^2+336u_2u_1+132u_2^2)\eta^3+(1575Qu_1+210Qu_2)\eta^2+1260Q^2\eta]\eta_{xx}\\
&\quad+[(63u_1-42u_2)\eta^4+315Q\eta^3]u_{1xx}+[(42u_1+4u_2)\eta^4+42Q\eta^3]u_{2xx}\\
&\quad+((378u_1^2+336u_2u_1+120u_2^2)\eta^2+(-315Qu_1-42Qu_2)\eta-1260Q^2)(\eta_x)^2\\
&\quad+(((945u_1+294u_2)\eta^3+1575Q\eta^2)u_{1x}+((378u_1+252u_2)\eta^3+210Q\eta^2)u_{2x})\eta_x\\
&\quad-63\eta^4(u_{1x})^2-4\eta^4(u_{2x})^2+1890\eta^3+(1260u_1^2+336u_2^2)\eta^2-3780S\eta+3780Q^2=0,
\end{aligned}
\tag{4.27}
$$

$$
\begin{aligned}
&[(-63u_1^2-20u_2^2)\eta^4+(-252Qu_1+84Qu_2)\eta^3-315Q^2\eta^2]\eta_{xxx}+[24u_2\eta^5\\
&\quad-126Q\eta^4]u_{1xxx}-[12u_1\eta^5]u_{2xxx}+(((126u_1^2+240u_2u_1+24u_2^2)\eta^3+(945Qu_1\\
&\quad+294Qu_2)\eta^2+1575Q^2\eta)\eta_x+((-315u_1+18u_2)\eta^4-693Q\eta^3)u_{1x}+((-66u_1\\
&\quad-84u_2)\eta^4+126Q\eta^3)u_{2x})\eta_{xx}+(((-126u_1+72u_2)\eta^4-504Q\eta^3)\eta_x+12\eta^5u_{2x})u_{1xx}\\
&\quad+(((-72u_1-40u_2)\eta^4+84Q\eta^3)\eta_x-24\eta^5u_{1x})u_{2xx}+((126u_1^2+240u_2u_1\\
&\quad+72u_2^2)\eta^2+(-378Qu_1-84Qu_2)\eta-1260Q^2)(\eta_x)^3\\
&\quad+(((126u_1+300u_2)\eta^3+630Q\eta^2)u_{1x}+((132u_1+72u_2)\eta^3+252Q\eta^2)u_{2x})(\eta_x)^2\\
&\quad+(-252\eta^4(u_{1x})^2-96\eta^4u_{2x}u_{1x}-48\eta^4(u_{2x})^2+672u_2u_1\eta^2-1260Qu_1\eta)\eta_x\\
&\quad+(840u_2\eta^3+1260Q\eta^2)u_{1x}+504u_1\eta^3u_{2x}=0,
\end{aligned}
\tag{4.28}
$$

and

$$
\begin{aligned}
&[(477u_1^2+312u_2u_1+124u_2^2)\eta^4+(1323Qu_1+162Qu_2)\eta^3+1134Q^2\eta^2]\eta_{xxx}\\
&\quad+[(27u_1-42u_2)\eta^5+315Q\eta^4]u_{1xxx}+[(42u_1+4u_2)\eta^5+18Q\eta^4]u_{2xxx}\\
&\quad+(((2214u_1^2+1728u_2u_1+584u_2^2)\eta^3+(2079Qu_1+882Qu_2)\eta^2-1890Q^2\eta)\eta_x\\
&\quad+((1773u_1+522u_2)\eta^4+2772Q\eta^3)u_{1x}+((654u_1+476u_2)\eta^4+288Q\eta^3)u_{2x})\eta_{xx}\\
&\quad+(((954u_1+144u_2)\eta^4+1953Q\eta^3)\eta_x-27\eta^5u_{1x}-42\eta^5u_{2x})u_{1xx}\\
&\quad+(((480u_1+248u_2)\eta^4+198Q\eta^3)\eta_x+42\eta^5u_{1x}-4\eta^5u_{2x})u_{2xx}\\
&\quad+((270u_1^2+432u_2u_1+168u_2^2)\eta^2+(-756Qu_1-360Qu_2)\eta+756Q^2)(\eta_x)^3\\
&\quad+(((2826u_1+1188u_2)\eta^3+1512Q\eta^2)u_{1x}+((1212u_1+856u_2)\eta^3\\
&\quad+576Q\eta^2)u_{2x})(\eta_x)^2+(684\eta^4(u_{1x})^2+480\eta^4u_{2x}u_{1x}+208\eta^4(u_{2x})^2+3780\eta^3\\
&\quad+(756u_1^2+432u_2^2)\eta^2-1008\mathrm{Qu}_2\eta-3780Q^2)\eta_x+3024u_1\eta^3u_{1x}\\
&\quad+(960u_2\eta^3+1008Q\eta^2)u_{2x}=0.
\end{aligned}
\tag{4.29}
$$

The velocity field is given by

$$v^1=u_0+u_1s+u_2s^2, \tag{4.30a}$$

$$v^3=w_0+w_1s+w_2s^2+w_3s^3, \tag{4.30b}$$

where

$$u_0=Q/\eta-\tfrac{1}{3}u_2, \tag{4.31a}$$

$$w_0=\tfrac{1}{2}Q(\eta_x/\eta)-\tfrac{1}{6}u_2\eta_x+\tfrac{1}{4}u_1\eta_x+\tfrac{1}{4}u_{1x}\eta, \tag{4.31b}$$

$$w_1=\tfrac{1}{2}Q(\eta_x/\eta)+\tfrac{1}{2}u_1\eta_x+\tfrac{1}{6}u_{2x}\eta, \tag{4.31c}$$

$$w_2=\tfrac{1}{2}u_2\eta_x+\tfrac{1}{4}u_1\eta_x-\tfrac{1}{4}u_{1x}\eta, \tag{4.31d}$$

$$w_3=\tfrac{1}{3}u_2\eta_x-\tfrac{1}{6}u_{2x}\eta. \tag{4.31e}$$

From (4.30) and (4.31) it follows that the vorticity distribution is given by

$$\begin{aligned}\Omega = &-[\{4u_2\eta^2\eta_{xx}-12u_2\eta(\eta_x)^2+8u_{2x}\eta^2\eta_x-2u_{2xx}\eta^3\}s^3\\&+\{(6u_2+3u_1)\eta^2\eta_{xx}+(-24u_2-6u_1)\eta(\eta_x)^2+(12u_{2x}+6u_{1x})\eta^2\eta_x-3u_{1xx}\eta^3\}s^2\\&+\{(6\eta\eta_{xx}-12(\eta_x)^2)Q+6u_1\eta^2\eta_{xx}\\&+(-12u_2-12u_1)\eta(\eta_x)^2+12u_{1x}\eta^2\eta_x+2u_{2xx}\eta^3-48u_2\eta\}s\\&+(6\eta\eta_{xx}-12(\eta_x)^2)Q+(-2u_2+3u_1)\eta^2\eta_{xx}-6u_1\eta(\eta_x)^2\\&+(-4u_{2x}+6u_{1x})\eta^2\eta_x+3u_{1xx}\eta^3-24u_1\eta]/(12\eta^2).\end{aligned}\tag{4.32}$$

The algebra involved in obtaining the above equations is of course formidable, but is easily handled by computer programs capable of symbolic manipulation. The progam MACSYMA (developed at the Massachusetts Institute of Technology) was used extensively in this research.

4.4. *Linearized equations*

We now obtain linearized forms of the foregoing equations for a stream of undisturbed depth d. The linearized Theory I equation has been given previously by Green & Naghdi (1974) and is

$$c^2d^2h_{xx}+(3d-3c^2)h=0,\tag{4.33}$$

where h represents the height of a small steady disturbance relative to the still water level, and c is its speed of propagation.

Linearized forms of the governing equations for the second and third levels of approximation are obtained by setting $\eta(x)=d+h(x)$ in (4.24)–(4.25) and (4.27)–(4.29), respectively, where $h(x)$ and the velocity components u_n are assumed small, along with their derivatives. Retaining only first-order terms in small quantities, we obtain the following forms for the Theory II equations:

$$(-12S+18d^2)h+4dQ^2h_{xx}+d^3Qu_{1xx}-12(dS-Q^2)+6d^3=0,$$

and

$$-2d^4Qu_{1xxx}-5d^2Q^2h_{xxx}+20d^2Qu_{1x}=0.$$

Eliminating u_1 from these two equations yields the single equation

$$\begin{aligned}3d^3Q^2h_{xxxx}+(&-24d^2S-80dQ^2+36d^4)h_{xx}\\&+(240S-360d^2)h+240dS-240Q^2-120d^3=0.\end{aligned}\tag{4.34}$$

Consistent with the present assumption of a small disturbance, the integrated pressure may be taken to be hydrostatic and the flow velocities negligible compared with the velocity of wave propagation. Hence, the mass flow rate and momentum flux take on values appropriate to uniform flow,

$$Q=-cd,\quad S=c^2d+\tfrac{1}{2}d^2.$$

Using the above in (4.34), we obtain the linearized Theory II equation

$$3c^2d^4h_{xxxx}+(24d^3-104c^2d^2)h_{xx}+(-240d+240c^2)h=0.\tag{4.35}$$

A similar procedure applied to (4.27)–(4.29) yields a sixth-order linear equation for Theory III:

$$\begin{aligned}c^2d^6h_{xxxxxx}+(15d^5-135c^2d^4)h_{xxxx}+(&-780d^3+2880c^2d^2)h_{xx}\\&+(6300d-6300c^2)h=0.\end{aligned}\tag{4.36}$$

5. Solitary wave solutions

We now obtain solutions to the above equations, first considering the problem of a solitary wave. Before proceeding, we recall some previous results. Stokes (see Lamb 1932, p. 425) showed that the asymptotic solution for the wave profile is exponential, i.e.

$$h(x) \propto \mathrm{e}^{2\alpha x} \quad \text{as } x \to \pm\infty, \tag{5.1}$$

where h is the wave height above an undisturbed depth of unity and α, sometimes called the 'straining parameter', is a solution of the transcendental relationship

$$\frac{\tan 2\alpha}{2\alpha} = F^2, \tag{5.2}$$

where F is the depth Froude number. This result is exact for an ideal fluid.

Grimshaw (1971) was the first to carry out the Rayleigh–Boussinesq approximation to the third order for solitary waves. His solutions for the speed and surface profile of the solitary wave are given by Fenton (1972) in the non-dimensional form

$$F^2 = 1 + \epsilon - \tfrac{1}{20}\epsilon^2 - \tfrac{3}{70}\epsilon^3, \tag{5.3}$$

$$\alpha^2 = \tfrac{3}{4}\epsilon - \tfrac{15}{16}\epsilon^2 + \tfrac{9}{8}\epsilon^3, \tag{5.4}$$

$$\begin{aligned}\eta(x) = 1 + \epsilon[\operatorname{sech}^2(\alpha x)] + \epsilon^2[-\tfrac{3}{4}\operatorname{sech}^2(\alpha x)\tanh^2(\alpha x)] \\ + \epsilon^3[\tfrac{5}{8}\operatorname{sech}^2(\alpha x)\tanh^2(\alpha x) - \tfrac{101}{80}\operatorname{sech}^4(\alpha x)\tanh^2(\alpha x)],\end{aligned} \tag{5.5}$$

where ϵ is the wave height, $\eta(x)$ represents the profile measured from the bottom, and the undisturbed depth is taken to be unity. Like the exact solution, the asymptotic behaviour of this solution is exponential, where the term α is an approximation to the straining parameter as defined in (5.2). The solution (5.3)–(5.5) reduces to the second-order result of Laitone (1960) after dropping terms of $O(\epsilon^3)$, and to the first-order result of Boussinesq (1871) after dropping terms of $O(\epsilon^2)$.

In figure 2 Stokes' relationship between straining parameter and Froude number is plotted, along with the predictions from the first three orders of shallow-water theory (given by (5.3) and (5.4)). We see that the agreement is good only for Froude numbers near unity, corresponding to waves of small height. Even at the third order, the results do not compare well beyond a Froude number $F \approx 1.10$, which corresponds to a wave-height of about $\epsilon \approx 0.2$, or less than one-fourth of the known maximum. It can also be seen that for Froude numbers near the maximum ($F_{\max} \approx 1.3$) the higher-order approximations diverge wildly. Using numerical methods, Fenton (1972) extended the perturbation solution to the ninth order. Although the range of validity increased with higher order, it was found that this erratic behaviour continued, all approximations eventually diverging within the regime of realistic wave speeds. Fenton was able to increase accuracy with the use of convergence-improvement techniques, but still was not able to predict the highest waves.

The direct theory predictions for the asymptotic wave profile are obtained from the linearized equations given in §4.4. We put $c = F$ and $d = 1$ in (4.33), (4.35) and (4.36) and assume solutions of the form $h = h_0\,\mathrm{e}^{2\alpha x}$. The resulting characteristic equations may be solved for F^2 and read

$$F^2 = \frac{1}{1 - \frac{4}{3}\alpha^2}, \tag{5.6a}$$

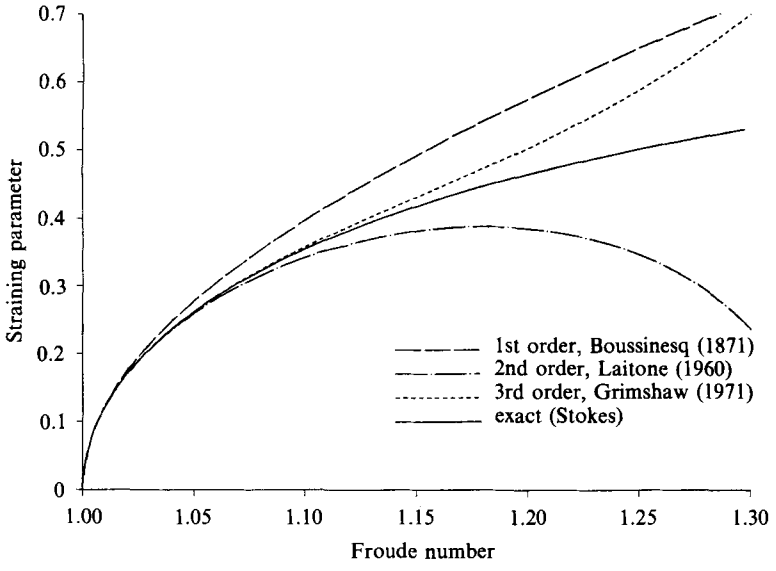

FIGURE 2. Variation of the straining parameter α with Froude number as predicted by the first three orders of classical shallow-water theory. Predictions are compared with Stokes' (exact) result.

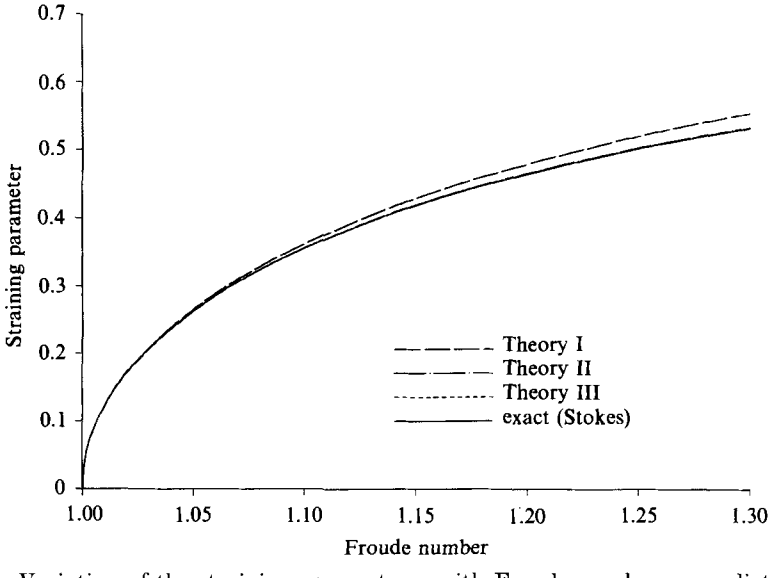

FIGURE 3. Variation of the straining parameter α with Froude number as predicted by the first three orders of the direct theory. Predictions of Theory II and Theory III cannot be distinguished from Stokes' result at this scale.

$$F^2 = \frac{1-\frac{2}{5}\alpha^2}{1-\frac{26}{15}\alpha^2+\frac{1}{5}\alpha^4}, \tag{5.6b}$$

and

$$F^2 = \frac{1-\frac{52}{105}\alpha^2+\frac{4}{105}\alpha^4}{1-\frac{64}{35}\alpha^2+\frac{12}{35}\alpha^4-\frac{16}{1575}\alpha^6}, \tag{5.6c}$$

for Theories I, II, and III, respectively.

In contrast to the perturbation results, the relationships between F and α predicted by the above equations, figure 3, are remarkably well behaved. Only the

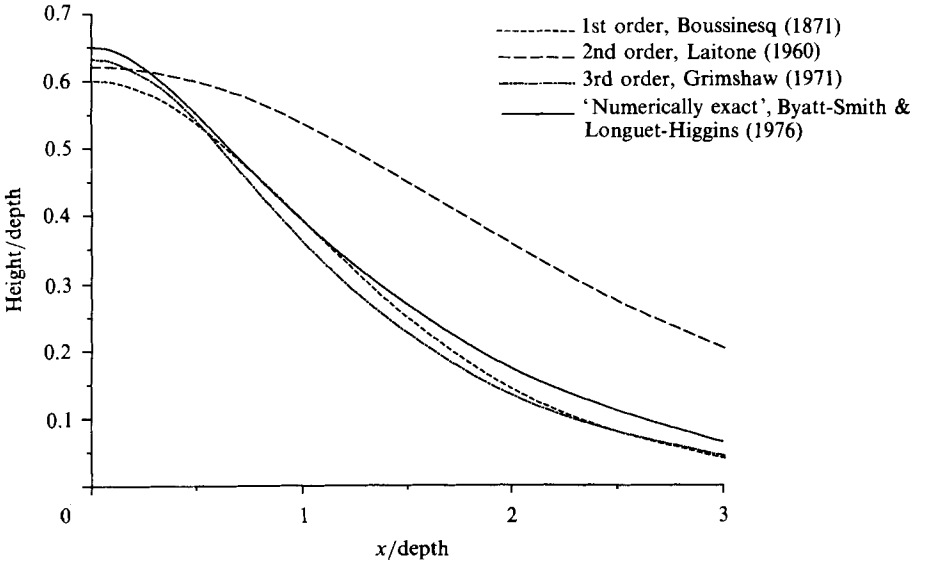

FIGURE 4. Surface profile of the solitary wave as predicted by the first three orders of classical shallow-water theory. Wave celerity is $F = 1.266$.

Theory I prediction differs significantly from the exact result; for Theory III the error is less than 10^{-5}, thus indistinguishable at this scale. Most importantly, all results seem to possess a uniform validity, with little increase in error as the Froude number increases.

This improvement might be attributed to the general superiority of the *rational approximants* for F^2 which arise from the direct theory, (5.6), as opposed to the *series approximations* one obtains from the perturbation methods, (5.3) and (5.4). In fact, it may be verified that (5.6*a*) is the [0, 2] Padé approximant to the exact relation for F^2 given in (5.2). Similarly (5.6*c*) is the [4, 6] Padé approximant to (5.2). Based on these results one might expect (5.6*b*) to be the [2, 4] Padé approximant; however this is not the case.

Let us now compare solutions of the full nonlinear equations. First, in figure 4 we plot the profile of a solitary wave of speed $F = 1.266$ predicted by the first-, second- and third-order shallow-water approximations and the numerically exact result for this Froude number (Byatt-Smith & Longuet-Higgins 1976). We note that the second-order result represents a substantial change from the first-order, and the third-order is a large change from this again; although it is not far from the first-order. Only at the wave crest does the solution appear to be converging regularly, increasing monotonically with higher order. The irregularity away from the crest is apparently related to the divergent behaviour of the straining parameter.

Figure 5 shows the result from direct theories I, II and III, and the numerically exact result (for the same Froude number). The Theory I solution is analytic and has been given previously by Green & Naghdi; it is identical to the solution of Rayleigh (1876). Solutions for Theories II and III were obtained numerically from the governing equations (4.24)–(4.25) and (4.27)–(4.29), respectively, using a finite-difference algorithm described in detail by Shields (1986). Here we see monotonic convergence not only at the crest but also far from the crest, reflecting the improved prediction for the straining parameter. For each successive level of approximation

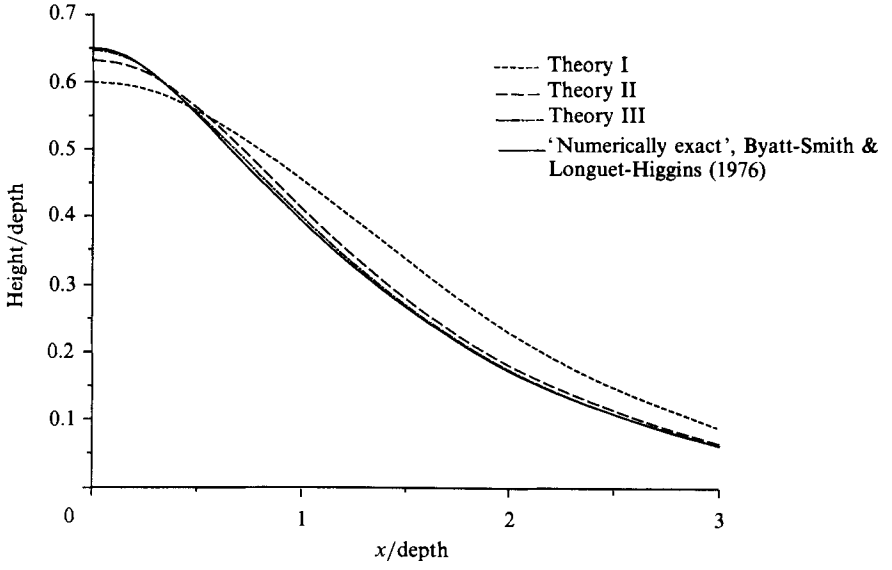

FIGURE 5. Surface profile of the solitary wave as predicted by the first three orders of the direct theory. Wave celerity is $F = 1.266$.

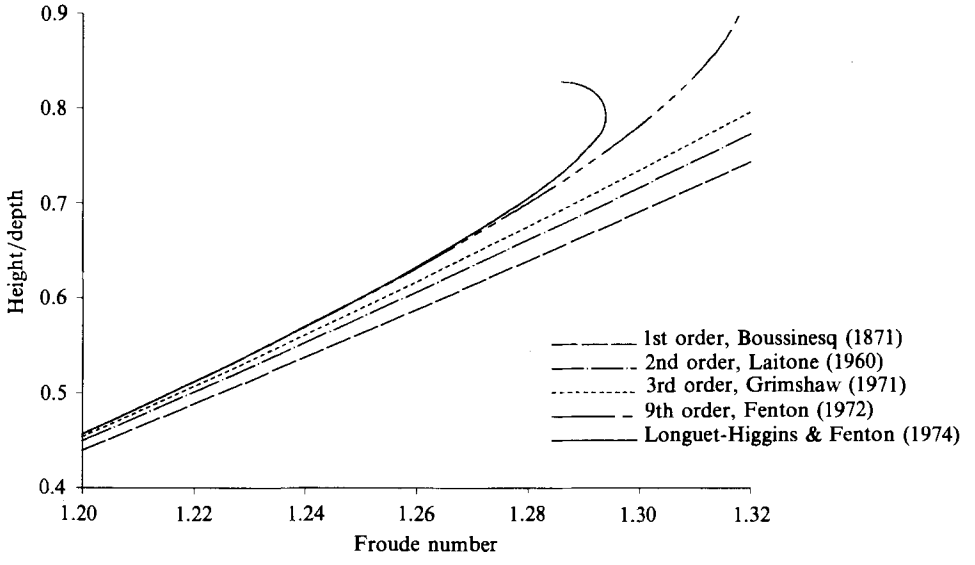

FIGURE 6. Relationship between solitary wave height and speed as predicted by various orders of classical shallow-water theory. Predictions are compared with the high-order numerical results of Longuet-Higgins & Fenton (1974).

the wave is higher and less broad. Note that the Theory II result represents a relatively small change to the Theory I result, with the Theory III prediction being a yet smaller change to this. The maximum difference in the profile shape between Theory III and the numerically exact result is less than 0.0048.

We now compare the various approximations to high-order numerical results. In figure 6 the relationship between wave height and speed given by Longuet-Higgins & Fenton (1974) is compared with that derived from the first-, second-, third-order perturbation theories, and also the (untransformed) ninth-order result of Fenton

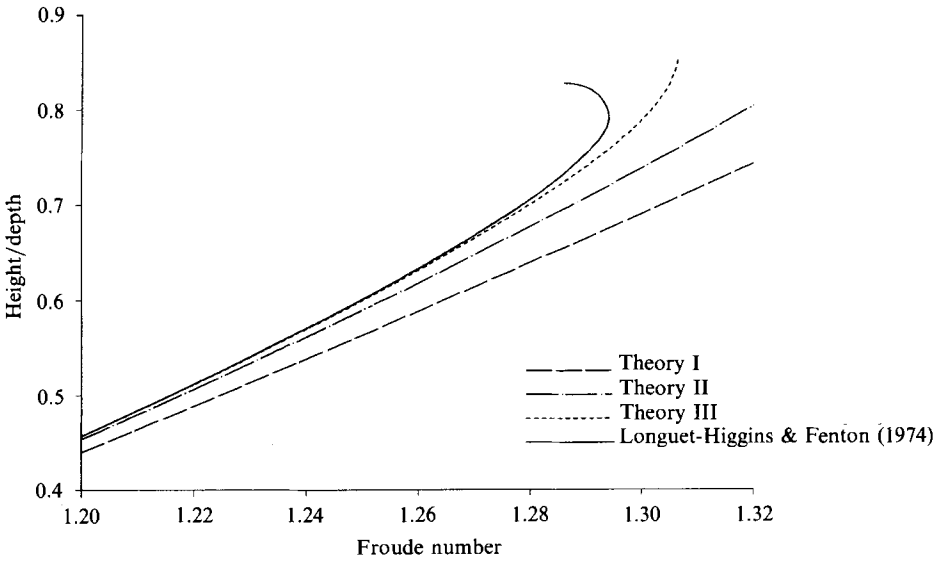

FIGURE 7. Relationship between solitary wave height and speed as predicted by the direct theory. Predictions are compared with the high-order numerical results of Longuet-Higgins & Fenton (1974).

(1972). There is a monotonic convergence towards the high-order result, although it is rather slow; even the ninth-order theory does not agree well beyond $F = 1.27$.

The same relationship is plotted in figure 7, this time giving the results from the direct theory. Clearly the direct theory converges much more rapidly to the high-order numerical result. In fact, Theory III is comparable in accuracy in the ninth-order perturbation solution. We also note that the Theory III result demonstrates a rapid upward curvature for higher Froude numbers, similar to the high-order numerical result. The curve terminates near $F = 1.31$, where wave height begins to increase rapidly with Froude number. The terminus of the curve represents a limit beyond which the numerical solution procedure would not converge. Similar behaviour was exhibited by Theory II, although the limiting Froude number was higher, about $F = 1.41$.

Near these values of F the Theory II and Theory III solutions were characterized by increasingly sharp crests, reminiscent of existing high-order numerical solutions and numerically exact solutions for the near-limiting wave. This behaviour seems related to certain singularities in the governing equations (4.24)–(4.25) and (4.27)–(4.29). Noting that these two systems of equations are linear in their highest-order derivatives, let us write them as two matrix equations of the form

$$\begin{bmatrix} c_{11} & c_{12} \\ c_{21} & c_{22} \end{bmatrix} \begin{bmatrix} \eta_{xxx} \\ u_{1xxx} \end{bmatrix} = \begin{bmatrix} d_1 \\ d_2 \end{bmatrix}, \tag{5.7}$$

for Theory II and, for Theory III

$$\begin{bmatrix} c_{11} & c_{12} & c_{13} \\ c_{21} & c_{22} & c_{23} \\ c_{31} & c_{32} & c_{33} \end{bmatrix} \begin{bmatrix} \eta_{xxx} \\ u_{1xxx} \\ u_{2xxx} \end{bmatrix} = \begin{bmatrix} d_1 \\ d_2 \\ d_3 \end{bmatrix}, \tag{5.8}$$

where the c_{ij} are the coefficients enclosed in square brackets in the governing

equations (4.24)–(4.25) and (4.27)–(4.29), respectively, and the d_j are the remaining terms. (In order to write the above forms it is formally necessary to first differentiate (4.24) and (4.27) with respect to x so that all equations are of the same order.) The determinant of the matrix in (5.7) is given by

$$c_{11}c_{22}-c_{12}c_{21} = -\eta^5(Q+u_1\eta)(15Q^2+10u_1\eta Q-u_1^2\eta^2), \tag{5.9}$$

and that in (5.8) is given by

$$\begin{aligned} &c_{11}(c_{22}c_{33}-c_{23}c_{32})-c_{12}(c_{21}c_{33}-c_{23}c_{31})+c_{13}(c_{21}c_{32}-c_{22}c_{31}) \\ &\quad = -48\eta^9(3Q+3u_1\eta+2u_2\eta)(-5292Q^3-1134u_2\eta Q^2-3969u_1\eta Q^2+504u_2^2\eta^2 Q \\ &\qquad +1008u_1u_2\eta^2 Q+1134u_1^2\eta^2 Q-8u_2^3\eta^3-84u_1u_2^2\eta^3+126u_1^2u_2\eta^3+567u_1^3\eta^3). \end{aligned} \tag{5.10}$$

Let us first consider the Theory II determinant, (5.9). Note that owing to the presence of the factor $(Q+u_1\eta)$ this determinant may vanish (and the equations may become singular) when $u_1\eta = -Q$. Consider now the horizontal fluid velocity at the surface of the wave for Theory II, $u_{\text{surface, II}}$. Recalling that the free surface is specified by $s=+1$, by (4.18a) and (4.22a) this may be written as

$$u_{\text{surface, II}} = \frac{Q}{\eta}+u_1. \tag{5.11}$$

According to the above, the condition $u_1\eta = -Q$ corresponds to $u_{\text{surface, II}} = 0$. Since our reference frame is translating with the wave, this condition implies an equivalence of surface-particle velocity and wave speed. Interestingly, this is the exact requirement for particle velocity at the crest of a limiting wave.

The horizontal component of the surface-fluid velocity corresponding to Theory III is obtained by setting $s=1$ in (4.30a) and using (4.31a). This is given by

$$u_{\text{surface, III}} = \frac{Q}{\eta}+u_1+\tfrac{2}{3}u_2. \tag{5.12}$$

Similar to Theory II, the Theory III determinant contains a factor $(3Q+3u_1\eta+2u_2\eta)$ which vanishes when this velocity is zero. Thus again we may identify a singularity in the system of equations with the criterion of a limiting wave. Furthermore, it is evident from the form of the governing equations of both theories that as these singularities are approached, the curvature of the solution for the wave profile becomes unbounded. This explains the cusp-like solutions that were observed.

This remarkable result is not present in Theory I, nor does it have any parallel in the comparable low-order perturbation theories. All of these latter theories yield analytic solutions, and these have no mathematical limitation for any choice of $F \geqslant 1$. From the results for Theory II and Theory III, we conjecture that all levels of the general theory for $K > 1$ contain a singularity associated with the limiting wave.

Further light may be shed on this feature by considering a certain non-dimensional parameter ω. This parameter, introduced by Longuet-Higgins & Fenton (1974), is defined by

$$\omega = 1-\frac{[U_{\text{crest}}]^2}{gd}, \tag{5.13}$$

where U_{crest} is the (dimensional) particle velocity at the wave crest, measured in wave-fixed coordinates. With this definition, ω increases monotonically from 0 to 1 as the wave amplitude varies from the infinestimal to its limiting value. Predictions

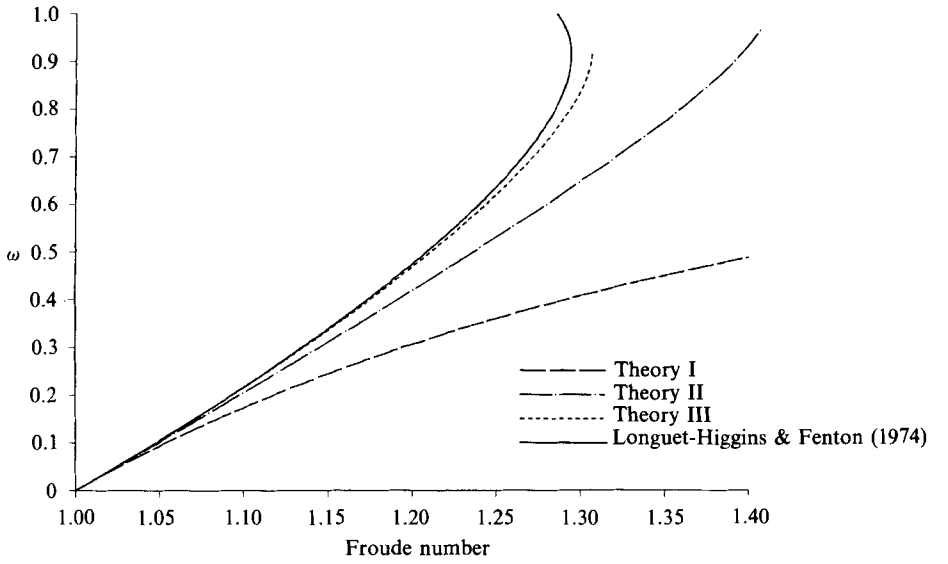

FIGURE 8. Variation of the parameter $\omega = 1 - U^2/gd$ with Froude number. The results of Longuet-Higgins & Fenton (1974) are compared with the predictions of the direct theory.

for ω from the direct theories are plotted against Froude number in figure 8, along with the results of Longuet-Higgins & Fenton (1974). We note a rapid convergence for the successive direct theories. The results from Theory II and Theory III demonstrate upward curvature throughout the range of F, tending toward the upper limit $\omega = 1$ at a finite value of Froude number. In contrast, it may be shown that the prediction of Theory I approaches the limit $\omega = 1$ asymptotically as $F \to \infty$.

The curves for Theories II and III terminate where the numerical solution procedure would no longer converge. Clearly, for Theory III this point corresponds to a rapid increase in ω with F. This occurs near $\omega = 0.9$, agreeing well with Longuet-Higgins & Fenton (1974). It is possible that the equations might yield two solutions for a certain range of wave speed, but this has yet to be verified. However, in addition to the wave speed, it is known that certain other wave properties reach maxima prior to the limiting wave. One in particular is the excess mass, defined as the non-dimensional fluid volume above the undisturbed free surface,

$$M = \int_{-\infty}^{+\infty} [\eta(x) - 1]\, dx. \tag{5.14}$$

Longuet-Higgins & Fenton (1974) found that this quantity, when plotted against ω, reaches a maximum before the maximum in Froude number is reached. In figure 9 we plot this relationship for the various direct approximations, along with the high-order numerical results. Note that Theory I predicts the mass to increase monotonically with ω, but the Theory II and Theory III results clearly attain maximum values, the latter being in excellent agreement with the results of Longuet-Higgins & Fenton (1974).

The foregoing results demonstrate that the theory is capable of predicting the 'gross' properties of solitary waves quite well. It is of interest now to consider other properties of the solutions. In particular, the derivation of the theory guarantees

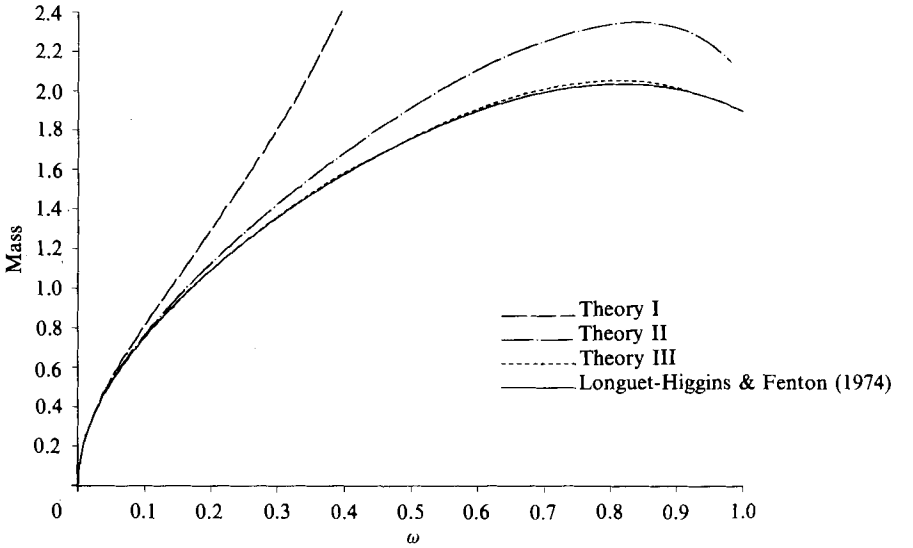

FIGURE 9. Excess mass of the solitary wave as a function of the parameter ω. Predictions of the direct theory are compared with the results of Longuet-Higgins & Fenton (1974).

that the predicted flow field is incompressible and that it satisfies kinematic boundary conditions. The situation with regard to vorticity in the flow is, however, different. In classical approaches the assumption is made that the flow started from an initially quiescent (irrotational) state and was produced by the action of conservative forces on the fluid. As a result of the Hankel–Kelvin theorem, the flow in this case will remain irrotational. One can show (Shields & Webster 1988) that it is possible to develop theorems similar in nature to the Hankel–Kelvin theorem for fluid sheets. These results show that: Theory I does not conserve any circulation across the sheet and is, in fact, fundamentally rotational; Theory II conserves a weighted average of circulation across the sheet; Theory III conserves two different weighted averages of circulation across the sheet, etc. The weighting functions are $(1-s^2), (1-s^2)\, s, \ldots$. As a result, the vorticity in a flow starting from rest does not remain zero (as in classical potential theory) but may become different from zero, as long as the corresponding weighted averages of the vorticity remain zero. Since all the weighting functions include the factor $(1-s^2)$, zero vorticity is best preserved near the midsurface of the fluid sheet and, in particular, the depth-averaged vorticity may not be zero.

The depth-integrated vorticity corresponding to the solitary wave solutions of figure 5 is plotted in figure 10. These results were calculated from the vorticity expressions corresponding to the three levels of approximation, given in (4.17), (4.26) and (4.32), respectively. We note that the error in each successive approximation is smaller, but that the improvement of Theory III over Theory II is not as large as one might expect, considering our earlier results for fundamental wave properties.

Noting that in all three cases the maximum error occurs under the wave crest, figure 11 shows the depth-distribution of vorticity at this location for each solution. As noted in §4.1, the vorticity of Theory I increases linearly from the bottom. The Theory II vorticity follows a parabolic distribution and is not necessarily zero at the bottom. Like Theory II, the vorticity distribution of Theory III seems to

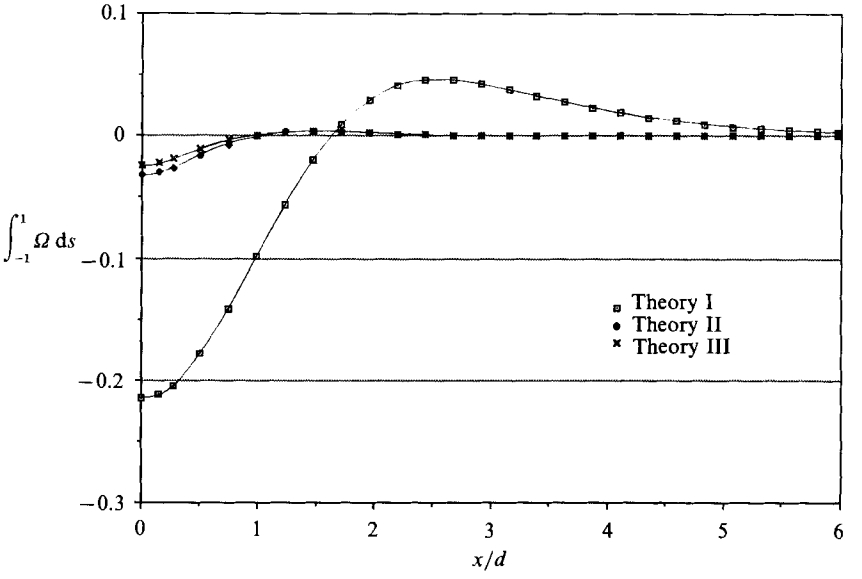

FIGURE 10. The distribution of depth-integrated vorticity as a function of the horizontal coordinate for the solitary wave solutions of figure 5 ($F = 1.266$). $x/d = 0$ corresponds to the wave crest.

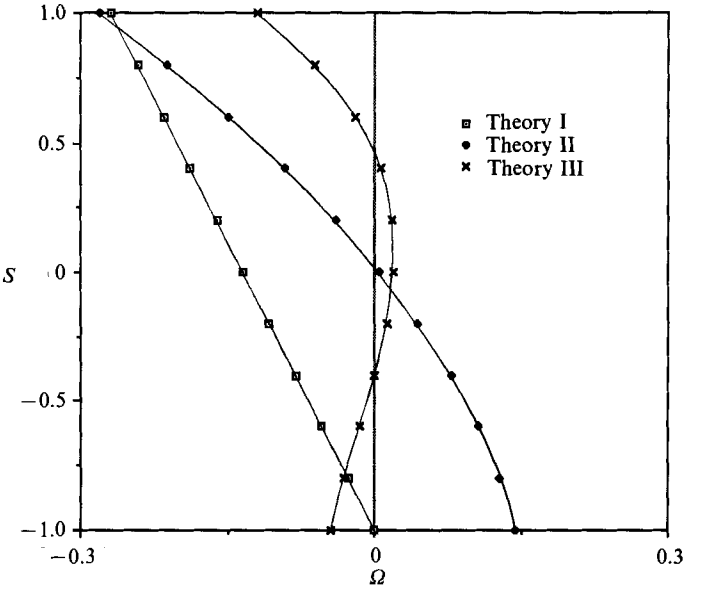

FIGURE 11. The depth-distribution of vorticity under the crests of the solitary wave solutions of figure 5. $s = 1$ corresponds to the wave surface; $s = -1$ corresponds to the bottom.

approximate a zero average value, but also has a smaller 'local' error; its maximum value is less than half of that of Theory II. These computed results are such that the applicable weighted moments of the vorticity are zero.

In summary, convergence towards irrotational flow is indicated in figures 10 and 11, but appears to be somewhat less rapid and lacking the monotonic character of the convergence for gross wave properties.

6. Periodic wave solutions

We now examine periodic waves, which is a larger undertaking since these are specified by two parameters rather than just one. Throughout this section we adopt the notation used by Cokelet (1977), choosing units of length such that the wavenumber is unity. Of immediate interest are the dispersion relationships for infinitesimal waves predicted by the direct theories. To obtain these, we seek a sinusoidal solution to the linearized equations of §4.4 by putting $h = h_0 e^{ix}$. Solving the resulting characteristic equations for the wave velocity, we obtain

$$c^2 = \frac{3d}{d^2+3}, \tag{6.1}$$

$$c^2 = \frac{24d^3+240d}{3d^4+104d^2+240}, \tag{6.2}$$

and

$$c^2 = \frac{15d^5+780d^3+6300d}{d^6+135d^4+2880d^2+6300}, \tag{6.3}$$

for Theories I, II, and III, respectively.

These results can be compared with Stokes' result, the familiar dispersion relation from linear wave theory. In the same non-dimensional variables, this is given by

$$c^2 = \tanh d. \tag{6.4}$$

Similar to the results obtained for the relationship between wave speed and the straining parameter for the solitary wave, (5.6), the relations (6.1) and (6.3) are Padé approximants to (6.4). Again the result for Theory II, (6.2), does not fit this pattern.

The above four relations are plotted in figure 12, using Cokelet's parametrization for the abscissa so that the entire range of depth/wavelength ratios is spanned. The exact result is unity at the deep-water limit (where $c^2 = g/k$), decreasing monotonically to zero at the shallow-water limit ($c^2 = gd$). All direct theories agree well for shallow water (i.e. long waves), and the range of validity is extended with increasing order, converging to the exact curve rapidly. In all cases the predicted celerity is positive for all finite water depths, but tends to zero as infinite depth is approached. The model is clearly inapplicable in the limiting deep-water case. However, it is at least physically reasonable for all finite water depths, and improves rapidly with increasing level of approximation.

It is important to note that the Theory III curve in figure 12 is accurate until very near the deep-water limit, attaining a maximum value just less than unity. This indicates that Theory III may be capable of modelling waves that are essentially deep-water waves, feeling very little effect from the bottom. The peak of the Theory III curve occurs for a depth-to-wavelength ratio of about 1:2, well beyond the range usually considered appropriate for a shallow-water approximation. For example, Fenton (1979) recommends against the use of even high-order cnoidal theory for waves shorter than 8 times the water depth, or $e^{-dk} \approx 0.46$ in figure 12.

Before attempting solutions, we recall that the direct theory was derived without any statement concerning the rotationality of the flow. In general, steady flows of an inviscid fluid have no unique solution unless the vorticity is specified (unsteady flows require a specification of the vorticity at one instant in time). As discussed in §5, the fluid-sheet theory presented here does not preserve vorticity point-wise. As a result

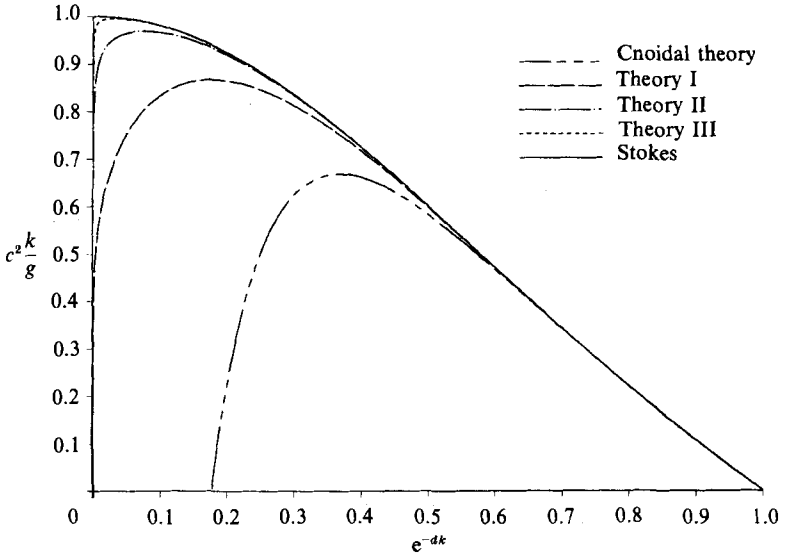

FIGURE 12. Dispersion relationship for infinitesimal waves. Predictions from Theories I, II and III are compared with the exact result.

of the analogue of the Hankel–Kelvin theorem for these flows (Shields & Webster 1988), an initially quiescent (irrotational) state implies only that the weighted average of the circulation around any segment of the fluid sheet be zero for Theory II and two such weighted averages be zero for Theory III.

We shall, however, approach the specification of vorticity from a different, but equivalent, point of view. Adopting Stokes' (1847) first definition of velocity for irrotational waves, we require that the horizontal velocity averaged over one wavelength at any fixed depth (below the level of the wave trough) is a constant. If this average is not independent of depth, the flow contains a net shear. A statement of this condition is given by

$$\int_0^\pi [c+u(x,z)]\,\mathrm{d}x \equiv 0, \tag{6.5}$$

for any z, where c is the velocity of propagation. Using the Theory III velocity field (4.21) in the above, we obtain

$$\int_0^\pi \left[c+\frac{Q}{\eta}-\tfrac{1}{3}u_2+u_1 s+u_2 s^2\right] = \mathrm{d}x = 0. \tag{6.6}$$

Recalling that $s = 2z/\eta - 1$, we have

$$\int_0^\pi \left[c+\frac{Q}{\eta}-u_1\right]\mathrm{d}x + 2z\int_0^\pi \frac{u_1-2u_2}{\eta}\,\mathrm{d}x + 4z^2\int_0^\pi \frac{u_2}{\eta}\,\mathrm{d}x = 0. \tag{6.7}$$

If the above expression is to hold for all values of z, all three integrals must vanish identically. Setting the second two integrals equal to zero can be shown to be exactly equivalent to the two vorticity constraints discussed above. Setting the first integral equal to zero defines the wave speed, c. The same process applied to Theory II yields a definition for the wave speed and the one vorticity constraint discussed in §5.

The solution procedure used the same finite-difference algorithm as was used for the solitary wave solutions, plus an iteration step to satisfy the above irrotationality

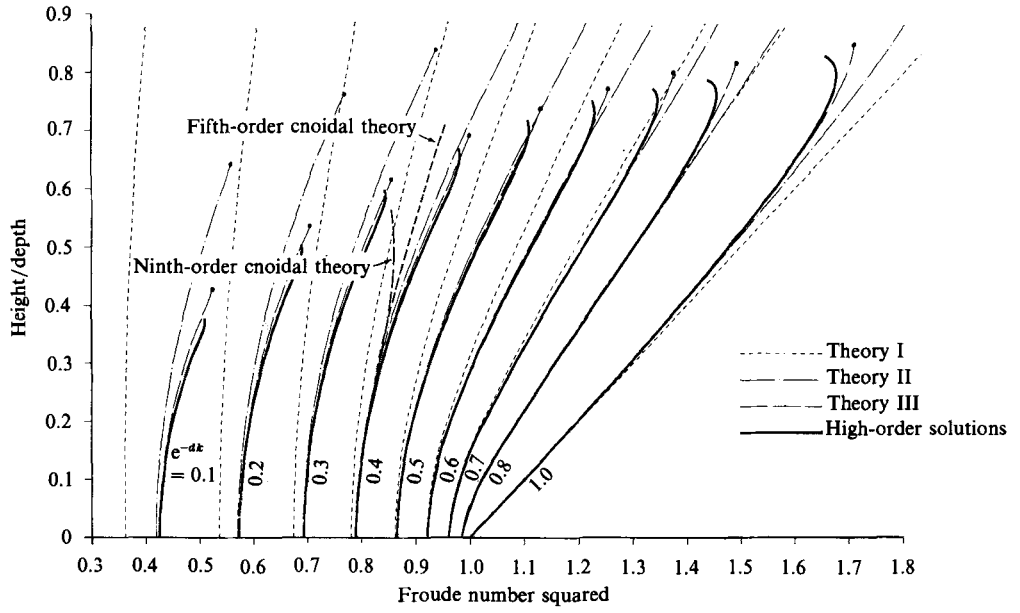

FIGURE 13. Relationship between wave height and wave speed squared for various ratios of depth to wavelength. Predictions of Theory III are compared with the periodic ($e^{-dk} < 1$) results of Cokelet (1977), and the solitary wave ($e^{-dk} = 1$) results of Longuet-Higgins & Fenton (1974). Dots ($\cdot$) indicate limiting wave heights predicted by the direct theory. Predictions from the fifth-order cnoidal theory of Fenton (1979) are shown for the one case $e^{-dk} = 0.4$.

constraints; details are given by Shields (1986). Figure 13 shows the resulting relationship between wave height and speed for various ratios of depth to wavelength. The definition of depth is that used by Cokelet (1977), i.e. $d = Q/c$. The predictions of Theories I, II and III are compared to the numerically exact results of Cokelet for periodic waves. Results of Longuet-Higgins & Fenton for the solitary wave extreme ($e^{-d} = 1.0$), are repeated for completeness. Rapid convergence of the direct theory is clearly demonstrated. Also, the limiting waves predicted by Theory III (indicated by dots ($\cdot$) at the points where the numerical solution failed) are in reasonably good agreement with the high-order numerical results.

Also sketched in this figure are the fifth- and ninth-order cnoidal solutions of Fenton (1979) for the single case $e^{-d} = 0.4$, taken directly from his figure 2. Breakdown of the cnoidal approximation is clearly evident; as Fenton noted, the solutions 'diverge disastrously' when the wave height and water depth both increase beyond a certain point. Asymptotic behaviour is also demonstrated, as the ninth-order prediction is worse than the fifth-order. In contrast, the third-level direct theory continues to yield good predictions, even for the essentially deep-water case of $e^{-d} = 0.1$, where $\lambda/d \approx 3$.

7. Concluding remarks

It is clear that the direct approach is superior to the Rayleigh–Boussinesq approach in its ability to predict fundamental wave properties for steady two-dimensional waves. The direct theory posesses a far greater range of applicability, extending from the solitary wave extreme to an essentially deep-water condition.

Wave peaking and limiting heights for steady waves are also predicted, and are implicit in the equations of the theory.

The approach does not incorporate an assumption of irrotational flow. As a result, solutions modelling irrotational waves generally contain non-zero vorticity. However, since an approximation is made to conservation of momentum, the solutions appear to minimize this vorticity as one proceeds to higher-order approximation.

With these findings, we conjecture that the general unsteady, three-dimensional equations from which these results are derived provide a more accurate model than could be obtained by the competing Rayleigh–Boussinesq approach. Unfortunately there is a great deal of algebraic complexity in the higher-level theories. In order to deal with such equations it seems that computer programs capable of symbolic manipulation are essential. It is the experience of the authors that with such a tool much progress can be made. Shields (1986) obtained the unsteady version of the Theory II equations (including arbitrary bottom topography) and used them in a numerical simulation of wave shoaling. It was found that the equations required very little additional computational effort relative to much simpler models, such as the Boussinesq-class equations of Wu (1981), and yielded solutions that agreed extremely well with experimental observations. Further research is currently underway along these lines, and will be reported elsewhere.

This research was sponsored by the Office of Naval Research under contract N000014-84-K-0026.

REFERENCES

ANTMAN, S. S. 1972 The theory of rods. In *Handbuch der Physik* (ed. S. Flügge), vol. VIa/2, pp. 641–703. Springer.

BENJAMIN, T. B. & LIGHTHILL, M. J. 1954 On cnoidal waves and bores. *Proc. R. Soc. Lond.* A **224**, 448–460.

BOUSSINESQ, J. 1871 Théorie de l'intumescence liquide appelée onde solitaire ou de translation se propageant dans un canal rectangulaire. *C. R. Acad. Sci. Paris* **72**, 755–759.

BOUSSINESQ, J. 1877 Essai sur la théorie des eaux courantes. *Mem. Divers Savants Acad. Sci. Inst. France, Sci. Math. Phys. Paris* **23**, 1–680; Additions et éclaircissements, **24**, 1–64.

BYATT-SMITH, J. G. B. & LONGUET-HIGGINS, M. S. 1976 On the speed and profile of steep solitary waves. *Proc. R. Soc. Lond.* A **350**, 175–189. (Numerical values for the curves presented in this paper provided by J. G. B. Byatt-Smith in a private communication, 1987.)

COKELET, E. D. 1977 Step gravity waves in water of arbitrary uniform depth. *Phil. Trans. R. Soc. Lond.* A **286**, 183–230.

DE, S. C. 1955 Contributions to the theory of Stokes waves. *Proc. Camb. Phil. Soc.* **51**, 713–736.

ERTEKIN, R. C. 1984 Soliton generation by moving disturbances in shallow water. Ph.D. thesis, University of California, Berkeley. v+352 pp.

ERTEKIN, R. C., WEBSTER, W. C. & WEHAUSEN, J. V. 1984 Ship-generated solitons. *Proc. 15th Symp. Naval Hydrodynam., Hamburg*, pp. 347–361, disc. 361–364.

ERTEKIN, R. C., WEBSTER, W. C. & WEHAUSEN, J. V. 1986 Waves caused by a moving disturbance in a shallow channel of finite width. *J. Fluid Mech.* **169**, 275–292.

FENTON, J. D. 1972 A ninth-order solution for the solitary wave. *J. Fluid Mech.* **53**, 237–246.

FENTON, J. D. 1979 A high-order cnoidal wave theory. *J. Fluid Mech.* **94**, 129–161.

FENTON, J. D. 1985 A fifth-order Stokes theory for steady waves. *J. Waterway, Port, Coastal and Ocean Engng, ACSE* **111**, 216–234.

GREEN, A. E., LAWS, N. & NAGHDI, P. M. 1974 On the theory of water waves. *Proc. R. Soc. Lond.* A **338**, 43–55.

GREEN, A. E. & NAGHDI, P. M. 1976 Directed fluid sheets. *Proc. R. Soc. Lond.* A **347**, 447–473.

GREEN, A. E. & NAGHDI, P. M. 1977 Water waves in a non-homogeneous incompressible fluid. *Trans. ASME* E: *J. Appl. Mech.* **44**, 523–528.

GREEN, A. E. & NAGHDI, P. M. 1984 A direct theory of viscous fluid flow in channels. *Arch. Rat. Mech. Anal.* **86**, 39–63.

GRIMSHAW, R. 1971 The solitary wave in water of variable depth. Part 2. *J. Fluid Mech.* **86**, 415–431.

KANTOROVICH, L. V. & KRYLOV, V. I. 1958 *Approximate Methods of Higher Analysis.* P. Noordhoff Ltd. (Groningen, The Netherlands 1964), 681 pp.

LAITONE, E. V. 1960 The second approximation to cnoidal and solitary waves. *J. Fluid Mech.* **9**, 430–444.

LAMB, H. 1932 *Hydrodynamics*, 6th edn. Cambridge University Press, 1932 (Dover, New York, 1945), 738 pp.

LEVICH, V. G. & KRYLOV, V. S. 1969 Surface-tension-driven phenomena. *Ann. Rev. Fluid Mech.* **1**, 293–316.

LONGUET-HIGGINS, M. S. & FENTON, J. D. 1974 On the mass, momentum, energy and circulation of a solitary wave. II. *Proc. R. Soc. Lond.* A **340**, 471–493.

MADSEN, O. S. & MEI, C. C. 1969 The transformation of a solitary wave over an uneven bottom. *J. Fluid Mech.* **39**, 781–791.

MILES, J. W. 1979 On the Korteweg–de Vries equation for a gradually varrying channel. *J. Fluid Mech.* **91**, 181–190.

MILES, J. W. & SALMON, R. 1985 Weakly dispersive, nonlinear gravity waves. *J. Fluid Mech.* **157**, 519–531.

NAGHDI, P. M. & RUBIN, M. B. 1981*a* On the transition to planing of a boat. *J. Fluid Mech.* **103**, 345–374.

NAGHDI, P. M. & RUBIN, M. B. 1981*b* On inviscid flow in a waterfall. *J. Fluid Mech.* **103**, 375–387.

NAGHDI, P. M. & VONGSARNPIGOON, L. 1986 The downstream flow beyond an obstacle. *J. Fluid Mech.* **162**, 223–236.

PEREGRINE, D. H. 1967 Long waves on a beach. *J. Fluid Mech.* **27**, 815–827.

RAYLEIGH, LORD 1876 On waves. *Phil. Mag.* **1**, 257–279, Scientific Paper, vol. 1, pp. 251–271.

SCHWARTZ, L. W. 1974 Computer extension and analytic continuation of Stokes' expansion for gravity waves. *J. Fluid Mech.* **62**, 553–578.

SHIELDS, J. J. 1986 A direct theory for waves approaching a beach. Ph.D. thesis, University of California, Berkeley, iii + 137 pp.

SHIELDS, J. J. & WEBSTER, W. C. 1988 Conservation of mechanical energy and circulation in the theory of inviscid fluid sheets. *J. Engng Maths* (in press).

SKJELBREIA, L. & HENDRICKSON, J. 1961 Fifth order gravity wave theory. *Proc. 7th Conf. Coastal Engng*, pp. 184–196.

STOKES, G. G. 1847 On the theory of oscillatory waves. *Trans. Camb. Phil. Soc.* **8**, 441–455.

SU, C. H. & MIRIE, R. M. 1980 On head-on collisions between two solitary waves. *J. Fluid Mech.* **98**, 509–525.

URSELL, F. 1953 The long-wave paradox in the theory of gravity waves. *Proc. Camb. Phil. Soc.* **49**, 685–694.

WHITHAM, G. B. 1967 Nonlinear dispersion of water waves. *J. Fluid Mech.* **27**, 399–412.

WU, T. Y. 1981 Long waves in ocean and coastal waters. *J. Engng Mech. Div. ASCE* **107**, EM3, pp. 501–522.